Appendix A (Niu *et al.*, 2011): All plots including those in the main text

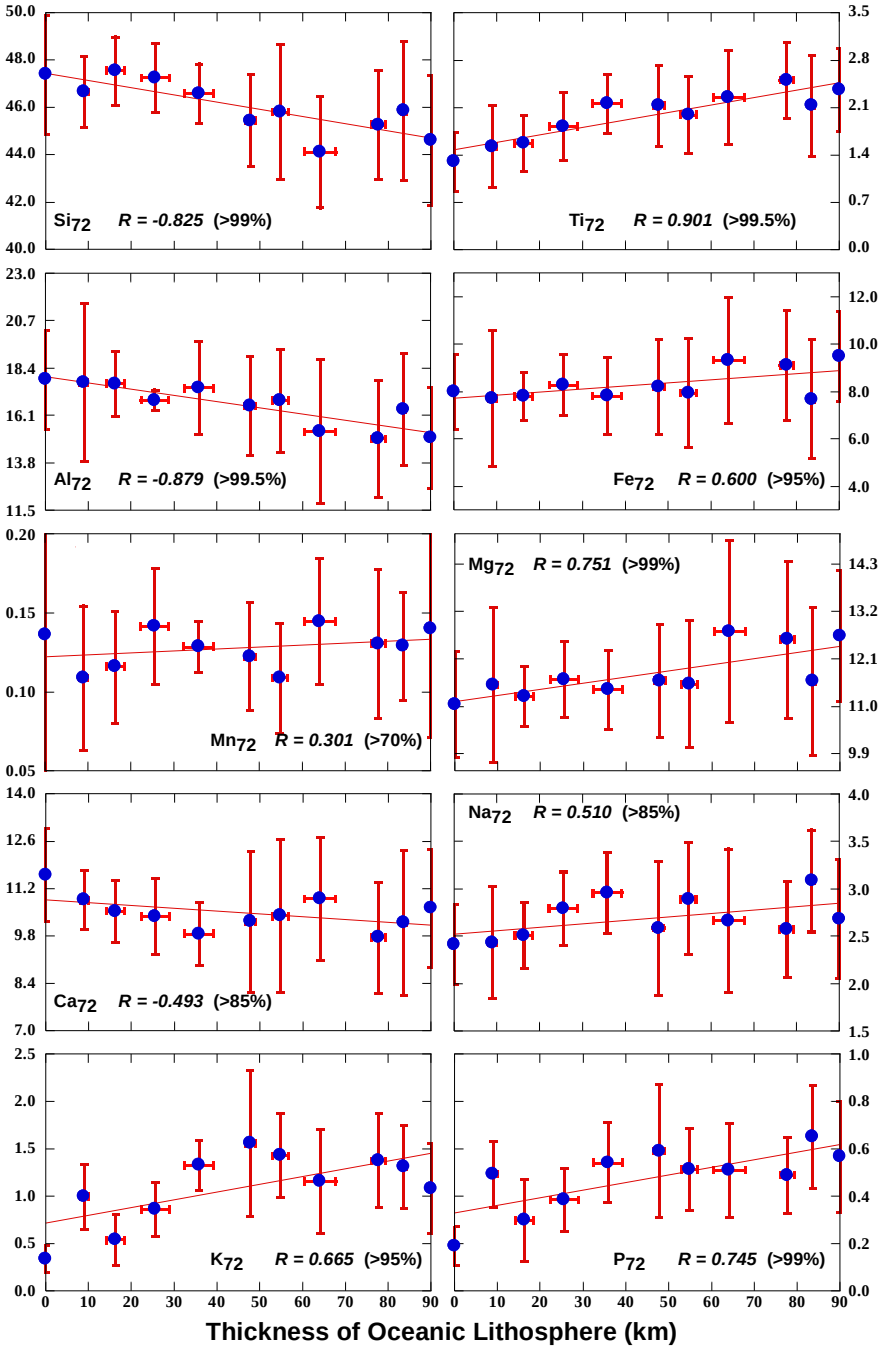

Fig. A1. Plots of average OIB major element oxides corrected for fractionation effect to $Mg^{\#}$ = 0.72 (Niu & O'Hara, 2008) as a function of lithosphere thickness using data in Table 1. Experimental studies (e.g., Jaques & Green, 1980; Walter, 1998) and modelling efforts (Niu & Batiza, 1991; Niu, 1997; Walter, 1998) show that SiO_2, Al_2O_3, FeO, MgO and CaO contents in mantle-derived melts depend on melting pressures. SiO_2 (strongly), Al_2O_3 (moderately) and CaO (weakly) decrease whereas MgO (strongly) and FeO (strongly/miderately) increase with increasing pressure of melting. Therefore, the decrease of mean Si_{72}, Al_{72} and Ca_{72} (weak) and increase of mean Mg_{72} and Fe_{72} in OIB with increasing lithosphere thickness at the time of OIB volcanism is consistent with increasing pressures of mantle melting from beneath thin lithosphere to beneath thickened lithosphere, i.e., the *lid effect*. On the other hand, predictably the abundances of incompatible element oxides such as TiO_2, Na_2O, K_2O and P_2O_5 in mantle melts must increase with decreasing extents of melting. Therefore, the increase of mean Ti_{72}, Na_{72} P_{72} and K_{72} in OIB with increasing lithosphere thickness at the time of OIB volcanism is consistent with decreasing extents of melting as the lithosphere thickens. Note that the rate of Na_{72} increase should be the same or more than that of Ti_{72} increase with increasing lithosphere thickness, but the fact that Na_2O becomes less incompatible with increasing melting pressure (Blundy *et al.*, 1995) compensate the effect of decreasing extent of melting towards beneath thickened lithosphere, which gives a weak Na_{72} trend. While melting in the garnet peridotite facies tend to have lower MnO in the melt relative to FeO, thus a weak decreasing Mn_{72} is expected, the lack of such a trend likely results from analytical errors for such a minor element and large mantle source heterogeneities (See text for details). The variably large 2σ error bars for each averaged data point is mostly caused by mantle source heterogeneities plus errors associated with fractionation effects (see Humphreys, 2009). Despite all these, the significant correlations between average OIB chemistry and lithosphere thickness attests that the oceanic lithosphere thickness exerts the primary control on the extents and pressures of mantle melting beneath volcanic islands and OIB chemistry, i.e., the *lid effect* (e.g., Niu & O'Hara, 2007; Humphreys & Niu, 2009; this study).

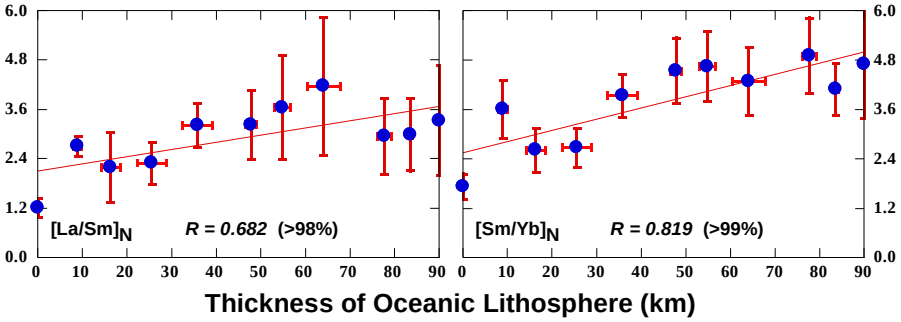

Fig. A2. Plots of average OIB rare earth element (REE) ratios La/Sm and Sm/Yb normalized (indicated by subscript "N") against Primitive mantle value (Sun & McDonough, 1989) as a function of lithosphere thickness using data in Table 1. As partition coefficients of REEs between major REE-host mantle minerals (i.e., clinopyroxene and garnet) and mantle melts increases systematically from light REE (e.g., La) to middle REE (e.g., Sm) and to heavy REE (e.g., Yb), the systematic increase in $[La/Sm]_N$ and $[Sm/Yb]_N$ ratios of OIB from volcanic islands on thin lithosphere to volcanic islands on thickened lithosphere is consistent with decreasing extents of mantle melting with increasing lithosphere thickness as indicated by incompatible elements in Fig. A1. Importantly, the REE partition coefficients between garnet and mantle melts vary over 2 orders of magnitude, so that whereas light REEs are incompatible in garnet, heavy REEs are strongly compatible in garnet (Irving & Frey, 1978). Consequently, high $[Sm/Yb]_N$ ratios in OIB would suggest the presence (and perhaps elevated abundances) of garnet as a residual phase in the mantle melting region that holds heavy REEs, i.e., the so-called "garnet signature" (melt contribution from melting under the garnet vs. spinel peridotite facies conditions). Therefore, the rather significant OIB $[Sm/Yb]_N$ increase with increasing lithosphere thickness reflects an increasing intensity of the "garnet signature". This is also consistent with increasing pressures of mantle melting from beneath thin lithosphere to beneath thickened lithosphere as indicated by major elements in Fig. A1 (e.g., Si_{72}, Al_{72}, Fe_{72} and Mg_{72}), and with decreasing extent of melting because the intensity of the "garnet signature" is diluted more (lower Sm/Yb) with increasing extent of melting beneath thin lithosphere where progressively more decompression melting occurs in the spinel peridotite facies.

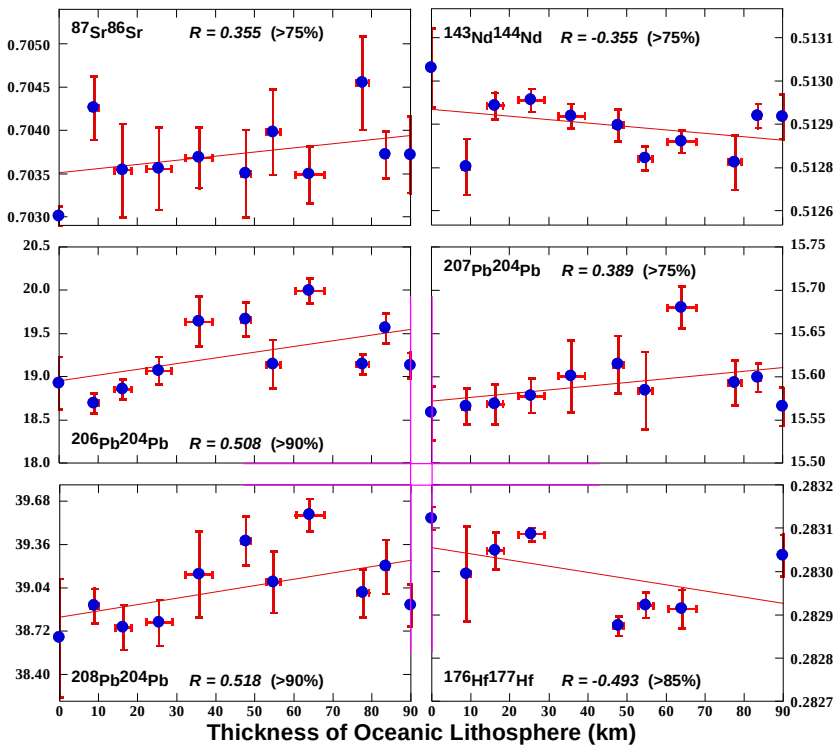

Fig. A3. Plots of average OIB radiogenic isotope ratios ($^{87}Sr/^{86}Sr$, $^{143}Nd/^{144}Nb$, $^{206}Pb/^{204}Pb$, $^{207}Pb/^{204}Pb$, $^{208}Pb/^{204}Pb$ and $^{176}Hf/^{177}Hf$) as a function of lithosphere thickness using data in Fig. A1. The weak trends for all these radiogenic isotopic ratios are consistent with lower extents of mantle melting with greater contributions of the more enriched source component towards beneath thickened lithosphere. That is, the *lid effect* is also discernible. However, the isotope data more faithfully reflect mantle source heterogeneities because the latter is independent of mantle melting conditions.

Fig. A4. Plots of average OIB radiogenic isotope ratios ($^{87}Sr/^{86}Sr$, $^{143}Nd/^{144}Nd$, $^{206}Pb/^{204}Pb$; $^{207}Pb/^{204}Pb$, $^{208}Pb/^{204}Pb$ and $^{176}Hf/^{177}Hf$) using data in Fig. A1. Significant coupling exists among Pb isotopes. Weak, but significant, Sr-Nd isotope coupling is also obvious. A weak Nd-Hf isotope coupling may exist. However, no obvious coupling exists between Hf and Sr isotopes. Certainly, Pb isotopes do not correlate in any way with Sr, Nd and Hf isotopes, which is, in fact, the primary observation that led to invoking mantle isotopic end-members (Zindler & Hart, 1986).

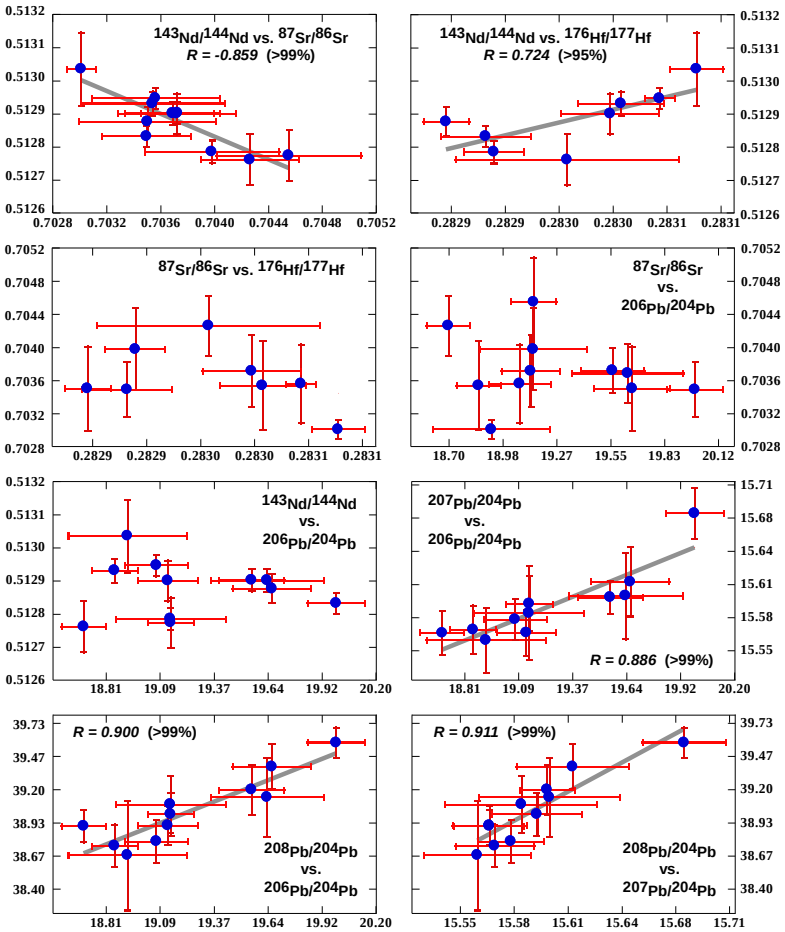

References:

Blundy, J. D., Falloon, T. J., Wood, B. J. & Dalton, J. A. (1995). Sodium partitioning between clinopyroxene and silicate melts. *Journal of Geophysical Research* **100**, 15501–15515.

Humphreys, E. R. & Niu, Y. L. (2009). On the composition of ocean island basalts (OIB): The effects of lithospheric thickness variation and mantle metasomatism. *Lithos* **112**, 118-136.

Irving, A. J. & Frey, F. A. (1978). Distribution of trace elements between garnet megacrysts and host volcanic liquids of kimberlitic to rhyolitic composition. *Geochimica et Cosmochimica Acta* **42**, 771-787.

Jaques, A. L. & Green, D. H. (1980). Anhydrous melting of peridotite at 0–15 kb pressure and the genesis of tholeiitic basalts. *Contributions Mineralogy and Petrology* **73**, 287–310.

MPI GEOROC data database (http://georoc.mpch-mainz.gwdg.de/georoc/).

Niu, Y. L. & O'Hara, M. J. (2007). Varying Ni in OIB olivines - product of process not source. *Geochimica et Cosmochimica Acta* **71**, a721-a721.

Niu, Y. L. & O'Hara, M. J. (2008). Global correlations of ocean ridge basalt chemistry with axial depth: A new perspective. *Journal of Petrology* **49**, 633-664.

Niu, Y. L. & Batiza, R. (1991). An empirical method for calculating melt compositions produced beneath mid, ocean ridges: Application for axis and off, axis (seamounts) melting. . *Journal of Geophysical Research* **96**, 21753-21777.

Niu, Y. L. (1997). Mantle melting and melt extraction processes beneath ocean ridges: Evidence from abyssal peridotites. *Journal of Petrology* **38**, 1047-1074.

Sun, S.-s. & McDonough, W. F. (1989). Chemical and isotopic systematics in ocean basalt. *Geological Society Specical Publication* **42**, 313-345.

Walter, M. J. (1998). Melting of Garnet Peridotite and the Origin of Komatiite and Depleted Lithosphere. *Journal of Petrology* **39**, 29-60.

Zindler, A. & Hart, S. R. (1986). Chemical geodynamics. *Annual Review of Earth and Planetary Sciences* **14**, 493–571.